

# Theory of $B_2O$ and $BeB_2$ Nanotubes: New Semiconductors and Metals in One Dimension

Peihong Zhang and Vincent H. Crespi

*Department of Physics and Materials Research Institute, The Pennsylvania State University, 104 Davey Lab,  
University Park, Pennsylvania 16802-6300*

(Received 9 February 2002; published 15 July 2002)

We describe two new boron-based nanotubes:  $B_2O$  and  $BeB_2$ . Both are isoelectronic to graphite, have reasonable curvature energies, and have already been made in their bulk planar forms. The lowest energy allotrope of planar single-layer  $B_2O$  is a semiconductor with a moderate band gap. The local density approximation band gap of the corresponding (3,0)  $B_2O$  nanotube [similar in size to (9,0) carbon nanotube tube] is direct and around 1.6 eV, within a range inaccessible to previous C or BN nanotubes. Single-layer  $BeB_2$  has a fascinating structure: the Be atoms rest above the boron hexagonal faces, nearly coplanar to the boron sheet. The unusual  $K$ -point  $\pi - \pi^*$  Fermi-level degeneracy of graphite survives, while a new nearly pointlike Fermi surface appears at the  $M$  point. As a result,  $BeB_2$  nanotubes are uniformly metallic.

DOI: 10.1103/PhysRevLett.89.056403

PACS numbers: 71.20.Tx, 61.48.+c, 61.72.Bb, 71.15.Ap

Carbon and boron nitride form two well-known classes of  $sp^2$ -bonded planar structures which can be rolled into cylinders with minimal energetic cost [1–4]. Within band theory, carbon tubes are metals or small-to-moderate gap semiconductors (roughly 1 eV or less), depending on the wrapping indices ( $n, m$ ). (These indices express the tube circumference in graphitic lattice coordinates.) Boron-nitride tubes, in contrast, are uniformly large-gap ( $\sim 5$  eV) semiconductors. Other tubular  $sp^2$  structures previously proposed include ordered alloys of boron, carbon, and nitrogen such as  $BC_3$  and  $BC_2N$ ; related multilayered structures have also been proposed [5]. Here we expand the scope of potential  $sp^2$  nanotubes by describing the theory of boron oxide and beryllium diboride nanotubes. These systems have unique electronic properties that are unattainable in the known systems. Both systems have already been produced in planar form, and we show that the energetic cost against curving them into tubes is less than that for carbon and boron nitride.

Planar  $B_2O$  and  $BeB_2$  are both isoelectronic to graphite and have been reported experimentally [6–8]. Conceptually,  $B_2O$  is graphite with one proton moved from each of two carbon nuclei onto a third to form an asymmetric sibling of graphitic carbon [6]. The difference in electronegativity between B and O is 1.5, only slightly larger than that between B and N. Therefore  $B_2O$  should also form strongly directional covalent bonds [6]. Similarly,  $BeB_2$  (in its  $AlB_2$  phase) can be conceptualized as graphite with one proton removed per carbon and placed in pairs above the centers of the hexagons (as a formal valence  $Be^{2+}$ ). These charge rearrangements, which do not damage the overall stability of the resulting structures, modify the electronic structure in substantial and interesting ways.

The destruction of sublattice symmetry in  $B_2O$  opens a band gap, but one smaller than that in BN. Surprisingly, two possible allotropes of  $B_2O$ , just slightly higher in energy than the semiconducting ground state, are metallic

within the local density approximation. The electronic structure of  $BeB_2$  is particularly fascinating: the graphitic sublattice symmetry remains, so the  $K$ -point degeneracy at the Fermi energy  $E_F$  survives. However, the perturbation to the crystal potential due to the Be atoms lowers the conduction band at the  $M$  point below  $E_F$ , so that the system sprouts three new nearly pointlike Fermi circles. Purely geometric band-folding arguments therefore suggest that, unlike carbon nanotubes, all  $BeB_2$  tubes are metallic (possibly with two different kinds of Fermi points). Density functional theory calculations on tubes confirm these geometrical expectations.

We use the *ab initio* pseudopotential method [9] in the local density approximation (LDA) to study the structural and electronic properties of these new classes of nanotubes. The energy cutoffs of the plane-wave expansions for  $B_2O$  and  $BeB_2$  are 120 and 60 Rydbergs, respectively. Brillouin zone  $k$ -point sampling grids are either  $8 \times 8 \times 1$  or  $10 \times 6 \times 1$  for planar structures, depending on the shape of the unit cells. The density of the  $k$ -point sampling along the axial direction of the tubes is similar to that in the planar structures.

Figure 1 shows optimized structural models of planar  $B_2O$  with both in-plane and out-of-plane relaxations

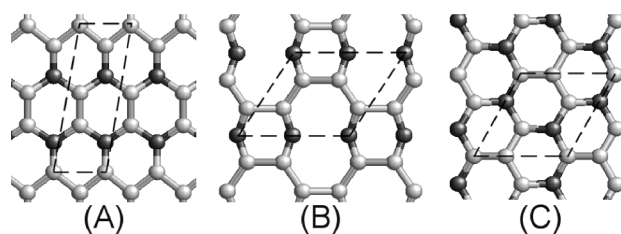


FIG. 1. Three alternative structural models of planar  $B_2O$ . Dark balls are oxygen; dashed lines show unit cells. Models A and B are metallic and are only slightly higher in energy than model C, which is a semiconductor.

TABLE I. Cohesive energies for the three models of single-layer  $B_2O$ , plus the cohesive energy of a (3, 0) nanotube based on model C.

Cohesive energy (eV/atom)			
Model A	Model B	Model C	(3, 0) nanotube
6.83	6.83	6.96	6.96

allowed. Table I shows the corresponding cohesive energies, plus the cohesive energy of the tubular allotrope shown in Fig. 2. Although each model starts from the ideal graphitic structure, only model C preserves hexagonal symmetry after relaxation. Out-of-plane relaxation is significant for C, much smaller for A, and essentially zero for B. The distance from the upper oxygen layer to the lower boron layer is about 1.5 a.u. for C and about 0.1 a.u. for A.

Model A was originally proposed by Hall and Compton for bulk  $B_2O$  [6]. We find this structure to be slightly higher in energy than model C (about 0.13 eV/atom), at least for the single-layer structure. The cohesive energy of B is 6.83 eV/atom, which is very close to that of A. Interestingly, the two higher energy models are metallic within the local density approximation, which is unexpected for a first-row covalent system with substantial ionicity. The lowest energy model, C, is a semiconductor with a valence band maximum at  $\Gamma$ . Unlike C, the metallic phases have continuous boron chains; these may form more robust delocalized  $p\pi$  bands and thereby explain the greater metallic character of these structures. Table II gives various bond lengths for the  $B_2O$  systems. Because of  $C_3$  symmetry, model C has only one type each of B – B and B – O bonds. Models A and C have very similar bond lengths, whereas model B has much shorter (and stronger) B – O bonds and correspondingly weaker B – B bonds due to the strong bond angle distortions around the oxygen atoms.

Since model C has the lowest energy, we focus on nanotubes of this structure. Figure 2 shows a relaxed (3, 0) nanotube with wrapping indices based on the unit cell of

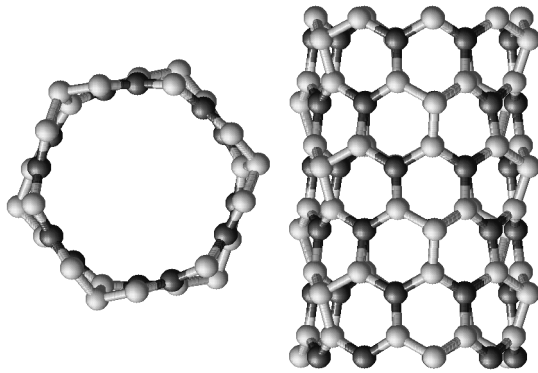


FIG. 2. A semiconducting (3, 0)  $B_2O$  nanotube. Dark balls are oxygen. The cross section appears hexagonal in projection due to an alternating bond angle distortion around boron atoms.

TABLE II. Bond lengths of the planar  $B_2O$  allotropes and the (3, 0) nanotube based on model C.

	Bond lengths (Å)			(3, 0) nanotube
	Model A	Model B	Model C	
B–B	~1.548–1.562	~1.651–1.717	1.541	~1.545–1.550
B–O	~1.449–1.453	1.338	1.470	~1.466–1.469

model C. The relatively weak B – B bonds buckle substantially in preference to the formation of a more planar B – O structure; this relaxation alternates in azimuthal position as one traverses the axis to produce the appearance in projection of a hexagonal cross section. Since buckling the relatively weak B – B bonds take less energy, the curvature energy of  $B_2O$  nanotubes is much smaller than that for corresponding homogeneous bonding systems such as carbon and boron nitride. Within density functional theory, the curvature energy of the (3, 0)  $B_2O$  nanotube [which is similar in diameter to a (9, 0) carbon nanotube] is nearly zero, possibly due to the shrinkage of the B – O bonds. For comparison, the curvature energies of carbon and boron-nitride tubes of similar diameter are 0.15 and 0.1 eV/atom, respectively. More precise calculations may reveal a small curvature energy.

Figure 3 compares the band structures of the semiconducting phase (model C) and a corresponding (3, 0) nanotube. Single-layer planar  $B_2O$  has a nearly direct band gap of about 2.8 eV (since this is an LDA band gap, it is likely underestimated). If the system is forced into perfect planarity, then this gap decreases substantially to 1.7 eV. This strong sensitivity to environment is also reflected in a large curvature-induced [10] band gap reduction: the band gap of the (3, 0) nanotube is only 1.63 eV and is direct at  $\Gamma$ . In contrast, the out-of-plane relaxation does not greatly perturb the LDA metallicity of models A or B in planar form. Since  $B_2O$  in model C has a high lattice symmetry,

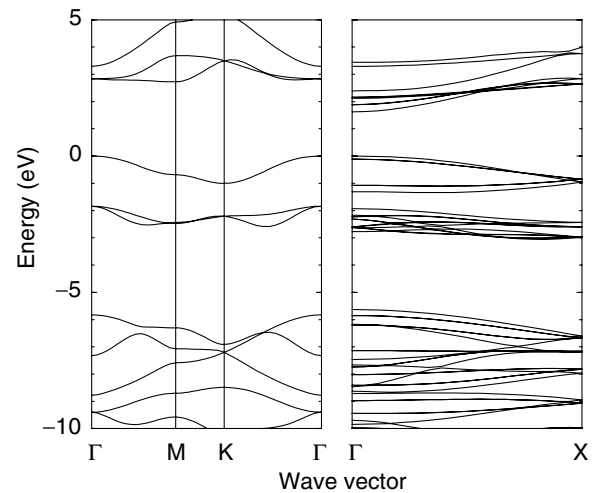


FIG. 3. Left panel: band structure of planar  $B_2O$ . Right panel: band structure of a (3, 0) nanotube with the same local structure.

we expect any curvature-induced out-of-plane distortions and the consequent perturbations to the band gap to be more strongly dependent on diameter than wrapping angle, although both may be important in sufficiently small-diameter tubes. This moderate (and at least in some cases, direct) band gap for  $\text{B}_2\text{O}$  nanotubes is potentially appealing for electronic or optical applications. The band gaps of corresponding carbon nanotubes are smaller and depend quite sensitively on both tube diameter and chirality, while the band gaps of boron-nitride nanotubes are larger, on the order of 5 eV.

In addition to these semiconducting  $\text{B}_2\text{O}$  tubes with almost isoenergetic metallic allotropes, boron can also form the basis for a uniformly metallic structure.  $\text{MgB}_2$  has recently received intense attention due to its high superconducting transition temperature [11] and its simple crystal structure (compared to oxide high  $T_c$  materials). Both  $\text{MgB}_2$  and the related material  $\text{BeB}_2$  assume the  $\text{AlB}_2$  structure (space group  $P6/mmm$ ), in which boron forms an AA-stacked graphitic hexagonal network with a Mg (Be) atom centered above each hexagon. These naturally layered structures motivate an investigation of single-layer  $\text{MgB}_2$  and  $\text{BeB}_2$  as possible archetypes for tubular structures. Table III compares the structural properties of single-layer and bulk  $\text{BeB}_2$  and  $\text{MgB}_2$  within LDA. Whereas the interlayer interaction (i.e., exfoliation energy) of  $\text{MgB}_2$  is large, that for  $\text{BeB}_2$  is only 0.1 eV/atom, just twice that in graphite [12].

The much lower surface energy of the Be-containing material arises from the smaller size of Be compared to Mg. Whereas the Mg atom in the single-layer compound rests high above the boron plane, the smaller Be atom drops from 1.40 Å above the boron layer (in the bulk) to only 0.50 Å above the plane in single-layer  $\text{BeB}_2$ , as shown in Fig. 4. The B–B bonds elongate accordingly, from 1.66 to 1.72 Å, to accommodate the nearly coplanar Be atom. Under appropriate conditions, single-layer  $\text{BeB}_2$  may coalesce in a tubular form. A multiwall tubular form might also maintain a smaller-than-bulk Be–B spacing due to the stacking frustration that arises from incommensuration between neighboring boron layers of different radii. Figure 4 shows the structure of a (5, 5)  $\text{BeB}_2$  nanotube. The Be atoms fall even closer to the B layer, within 0.44 Å. The curvature energy of the (5, 5)  $\text{BeB}_2$  nanotube is again very small, only about 0.05 eV/atom.

**TABLE III.** Structure properties of single-layer and bulk  $\text{BeB}_2$  and  $\text{MgB}_2$ . Values in parentheses are for the bulk materials.

	Bond length B–B (Å)	B–(Be,Mg) layer distance (Å)	Interlayer interaction (eV/atom)
$\text{MgB}_2$	1.746 (1.742)	1.532 (1.711)	0.7
$\text{BeB}_2$	1.722 (1.662)	0.496 (1.398)	0.1

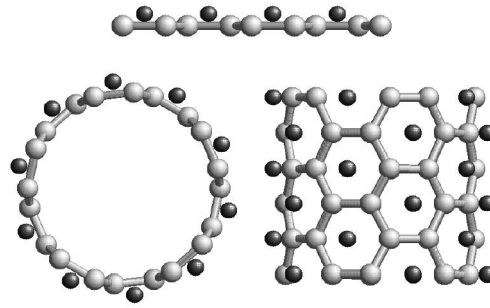


FIG. 4. Structure of single-layer  $\text{BeB}_2$  (top figure) and that of a (5, 5) nanotubes (bottom figures).

Figure 5 (left panel) shows the band structure of relaxed single-layer  $\text{BeB}_2$ . Graphene is well known for its unusual pointlike Fermi surface at the  $K$  points.  $\text{BeB}_2$  retains this fascinating low-energy idiosyncrasy and adds a second one: the  $\pi$  band at  $M$  apparently drops below  $E_F$  and produces three new nearly pointlike Fermi circles. Straightforward band-folding arguments then suggest that all  $\text{BeB}_2$  nanotubes are metallic. Does curvature-induced rehybridization in nanotubes remove these degeneracies? Curvature can actually enhance the metallicity: density functional calculations (see Fig. 6) show that the (5, 5) and (8, 0)  $\text{BeB}_2$  tubes are both metallic, with several bands crossing  $E_F$ .

The simple band-folding picture is complicated by substantial curvature-induced shifts in the band structure, as clarified by a study of the single-layer structure with the Be atoms pressed into the boron plane. The three lowest conduction bands at  $\Gamma$  have strong Be  $p$  character (two bands have mixed  $p_x$  and  $p_y$  character and the third is predominantly  $p_z$ ). In the optimized structure, the  $p_{xy}$  and

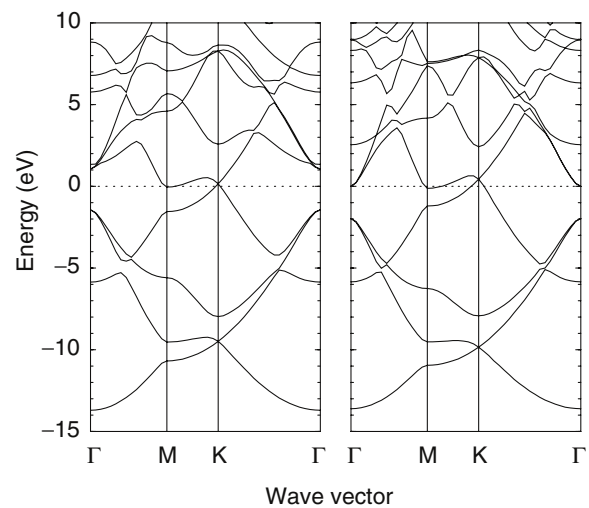


FIG. 5. Band structures of single-layer  $\text{BeB}_2$ . Left panel: in the relaxed structure. Right panel: with Be atoms forced into the same plane as the B atoms. The conduction bands at  $\Gamma$  of  $p_{x,y}$  character drop to the Fermi level.

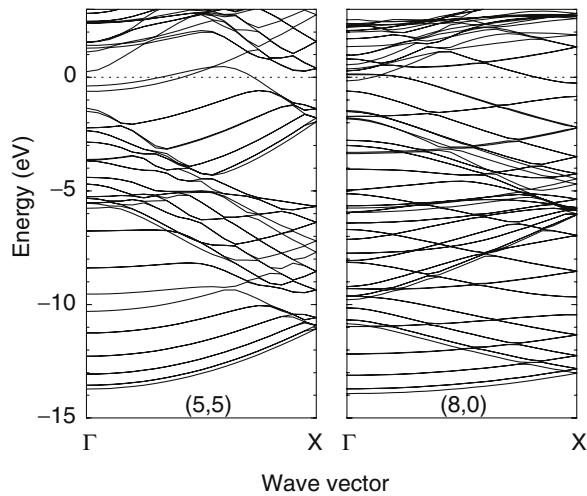


FIG. 6. Band structures of (5,5) and (8,0) BeB<sub>2</sub> nanotubes. Both are metallic.

$p_z$  bands are nearly degenerate at  $\Gamma$  and lie about 1 eV above  $E_F$ . When the Be atoms are pushed into the B layer, the energy of the  $p_{xy}$  bands at  $\Gamma$  drops to  $E_F$ , as shown in Fig. 5 (right panel). When the BeB<sub>2</sub> sheet curves into a tube, these same two bands also shift downwards and contribute to the uniform metallicity of the BeB<sub>2</sub> tubes. The outward bulging of these orbitals under curvature-induced rehybridization may enhance the band shifting effects of the Be atoms. At larger diameters, the simple band-folding picture should reassert itself. Figure 7 shows the density of states for (5,5) and (8,0) BeB<sub>2</sub> nanotubes. The densities of states at the Fermi level for both tubes are significantly higher than those for typical metallic carbon nanotubes. Note that distortions of the Be atoms could be softer than displacements of carbon in graphene sheets, so that the BeB<sub>2</sub> system may be more prone to Peierls-like

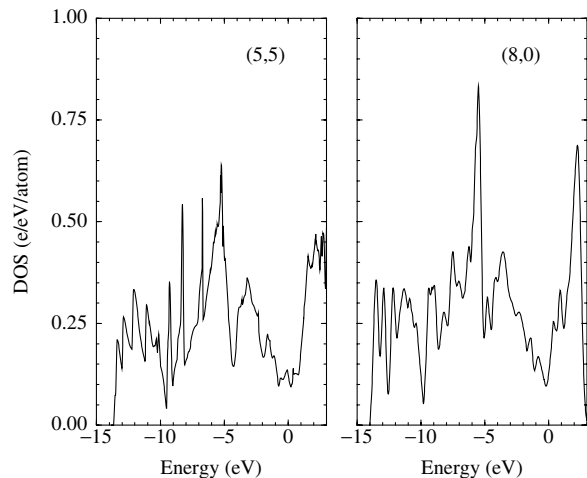


FIG. 7. The densities of states for (5,5) and (8,0) BeB<sub>2</sub> nanotubes in electrons per eV per boron atom. The Fermi level is shifted to 0 eV.

distortions, although multiple bands crossing the Fermi energy at different incommensurate wave vectors could not be gapped by a single low-period static distortion.

These two new classes of tubular structures promise to offer properties unavailable to the previously studied C, B, B – C – N, and B–N based systems. For example, B<sub>2</sub>O possesses an intermediate and relatively uniform semiconducting band gap and distinct chemical and physorption properties due to the presence of oxygen and boron and the highly buckled layers. The single-layer BeB<sub>2</sub> family, in addition to apparently being uniformly metallic (within a single-particle picture), offers the potential for large electron-phonon coupling matrix elements, relatively high density of states, and distinct surface reactivity and adsorption behavior due to the exposed metal atoms.

We gratefully acknowledge the support of the National Science Foundation (under Grant No. DMR-9876232), the Packard Foundation, and the Army Research Office.

- [1] S. Iijima, *Nature (London)* **354**, 56 (1991).
- [2] A. Rubio, J. L. Corkill, and M. L. Cohen, *Phys. Rev. B* **49**, 5081 (1994).
- [3] X. Blase, A. Rubio, S. G. Louie, and M. L. Cohen, *Europhys. Lett.* **28**, 335 (1994).
- [4] N. G. Chopra, R. L. Luyken, K. Cherrey, V. H. Crespi, M. L. Cohen, S. G. Louie, and A. Zettl, *Science* **269**, 966 (1995).
- [5] Z. Weng-Sieh, K. Cherrey, N. G. Chopra, X. Blase, Y. Miyamoto, A. Rubio, M. L. Cohen, S. G. Louie, A. Zettl, and R. Gronsky, *Phys. Rev. B* **51**, 11229 (1995); L. A. Chernozatonskii, *JETP Lett.* **74**, 335 (2001); I. Boustani, A. Quandt, E. Hernández, and A. Rubio, *J. Chem. Phys.* **110**, 3176 (1999); A. Quandt, A. Y. Liu, and I. Boustani, *Phys. Rev. B* **64**, 125422 (2001).
- [6] H. T. Hall and L. A. Compton, *Inorg. Chem.* **4**, 1213 (1965).
- [7] M. P. Grumbach, O. F. Sankey, and P. F. McMillan, *Phys. Rev. B* **52**, 15807 (1995).
- [8] Diamondlike forms have also been observed for B<sub>2</sub>O. T. Endo, T. Sato, and M. Shimada, *J. Mater. Sci. Lett.* **6**, 683 (1987). BeB<sub>2</sub>: L. Y. Markovskii, Y. D. Kondrashev, and G. V. Kaputovskais, *J. Gen. Chem. USSR* **25**, 1007 (1955); D. E. Sands, C. F. Cline, A. Zalkin, and C. L. Hoenig, *Acta Crystallogr.* **14**, 309 (1961); M. S. Borovikova and V. V. Fesenko, *J. Less Common Met.* **117**, 287 (1986).
- [9] J. Ihm, A. Zunger, and M. L. Cohen, *J. Phys. C* **12**, 4409 (1979).
- [10] X. Blase, L. X. Benedict, E. L. Shirley, and S. G. Louie, *Phys. Rev. Lett.* **72**, 1878 (1994).
- [11] J. Nagamatsu, N. Nakagawa, T. Muranaka, Y. Zenitani, and J. Akimitsu, *Nature (London)* **410**, 63 (2001).
- [12] This low interlayer interaction energy may be related to the more complicated layer stacking patterns seen in bulk BeB<sub>2</sub> (i.e., not purely AlB<sub>2</sub> stacking).